Vinculin phosphorylation differentially regulates mechanotransduction at cell–cell and cell–matrix adhesions

Jennifer L. Bays,[1] Xiao Peng,[1] Catlin E. Tolbert,[2] Christophe Guilluy,[2] Ashley E. Angell,[1] Yuan Pan,[1] Richard Superfine,[3] Keith Burridge,[2] and Kris A. DeMali[1]

[1]Department of Biochemistry, University of Iowa Roy J. Carver College of Medicine, Iowa City, IA 52242
[2]Departments of Cell Biology and [3]Physiology and Physics and Astronomy, University of North Carolina at Chapel Hill, Chapel Hill, NC 27599

Cells experience mechanical forces throughout their lifetimes. Vinculin is critical for transmitting these forces, yet how it achieves its distinct functions at cell–cell and cell–matrix adhesions remains unanswered. Here, we show vinculin is phosphorylated at Y822 in cell–cell, but not cell–matrix, adhesions. Phosphorylation at Y822 was elevated when forces were applied to E-cadherin and was required for vinculin to integrate into the cadherin complex. The mutation Y822F ablated these activities and prevented cells from stiffening in response to forces on E-cadherin. In contrast, Y822 phosphorylation was not required for vinculin functions in cell–matrix adhesions, including integrin-induced cell stiffening. Finally, forces applied to E-cadherin activated Abelson (Abl) tyrosine kinase to phosphorylate vinculin; Abl inhibition mimicked the loss of vinculin phosphorylation. These data reveal an unexpected regulatory mechanism in which vinculin Y822 phosphorylation determines whether cadherins transmit force and provides a paradigm for how a shared component of adhesions can produce biologically distinct functions.

Introduction

Cells are subjected to mechanical forces throughout their lifetimes. These forces include tension, compression, shear stress, swelling, and membrane curvature—all are consequences of normal physiological processes and can promote cell stiffening (Lessey et al., 2012; Plotnikov and Waterman, 2013). Modulation of its stiffness is critical for the cell to maintain the balance of forces between it and its surroundings. Perturbations in this balance between forces and stiffness underlies the etiology and progression of many diseases, including cancer, cardiovascular disease, diabetes, and others. Consequently much attention has focused on understanding mechanisms by which cells stiffen in response to forces. Studies of single cells have identified the critical cytoskeletal and signaling components. However, less is known about how groups of cells modulate their stiffness in response to mechanical forces.

External forces are sensed by cell surface adhesion receptors, including: (1) the cadherins, which bind to cadherins on neighboring cells to provide for strong cell–cell adhesion, and (2) the integrins, which establish and maintain the adhesion of cells to components of the ECM (Chen et al., 2004). Force transmission by integrins and cadherins share many striking similarities. In response to mechanical force, both integrins and cadherins: (1) cluster, (2) recruit a similar repertoire of proteins, and (3) initiate signaling cascades that culminate in activation of Rho family GTPases, particularly RhoA (Zhao et al., 2007; Goldyn et al., 2009; Guilluy et al., 2011). RhoA, in turn, regulates the activity of myosin II, which in conjunction with actin filaments allows cells to respond to mechanical stimuli by generating internal contractile forces (Chrzanowska-Wodnicka and Burridge, 1996). The net results can be cell stiffening, exerting traction on the surrounding matrix, and/or altering cell morphology. In addition to these similarities, forces on cadherins are propagated to integrin linkages with the ECM, and vice versa, suggesting that force transmission is highly integrated (Tsai and Kam, 2009; Borghi et al., 2012).

J.L. Bays and X. Peng contributed equally to this paper.

Correspondence to Kris A. DeMali: kris-demali@uiowa.edu

Abbreviations used in this paper: 3DFM, three-dimensional force microscopy; Abl, Abelson; WT, wild type.

The Rockefeller University Press $30.00
J. Cell Biol. Vol. 205 No. 2 251–263
www.jcb.org/cgi/doi/10.1083/jcb.201309092

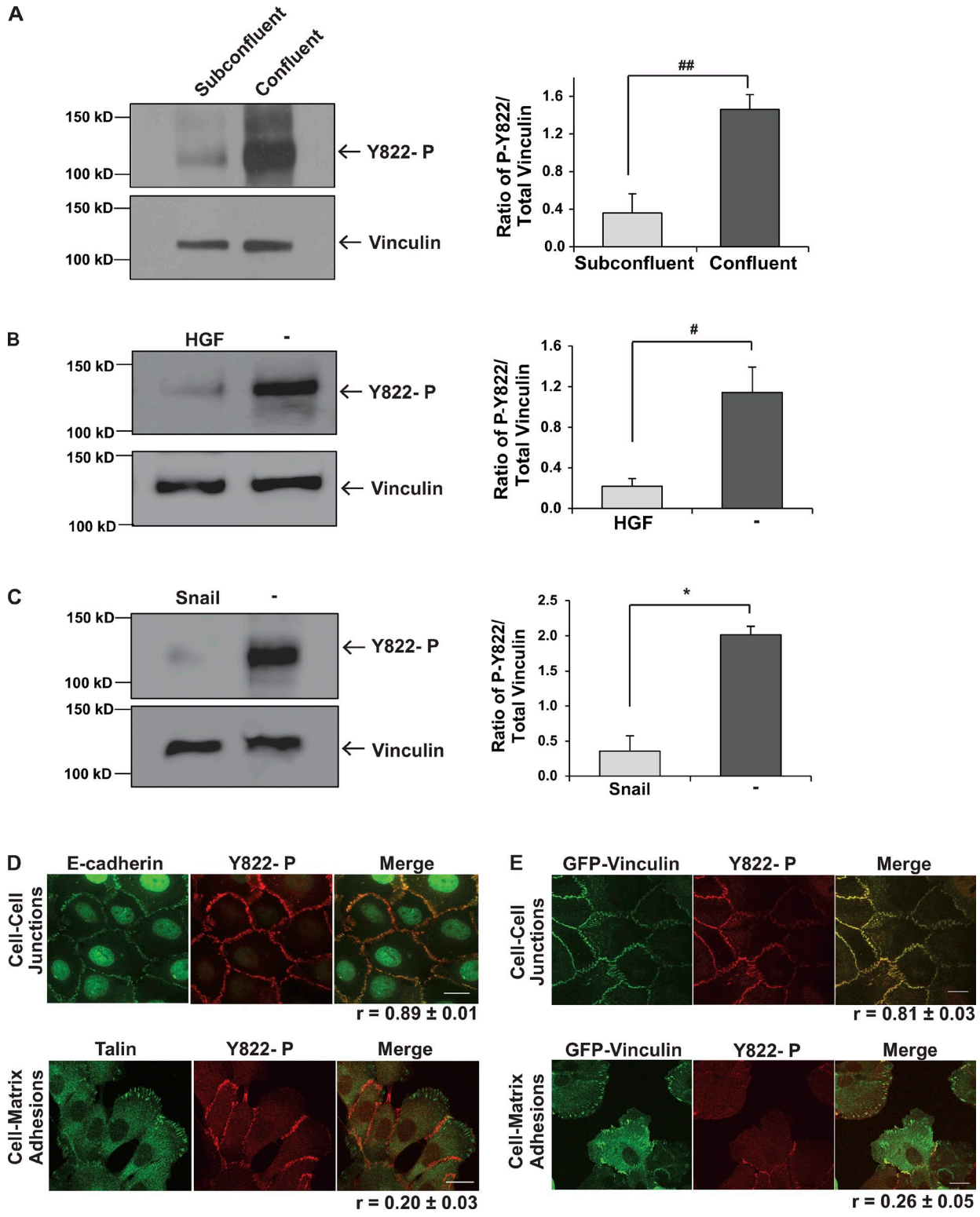

Figure 1. **Vinculin is specifically tyrosine phosphorylated at Y822 in cell–cell junctions.** (A) Effect of cell density on vinculin Y822 phosphorylation. Subconfluent or confluent cultures of MCF10a vinculin knockdown cells rescued with GFP-vinculin were lysed and immunoblotted with phosphospecific Y822 antibodies and stripped and reprobed for total vinculin levels. The left panel shows representative immunoblots and the right panel shows the quantification of the average amount of phosphorylated vinculin normalized to total vinculin levels from three independent experiments. ##, $P < 0.005$. (B and C) The effect of inducing an epithelial-to-mesenchymal transition on vinculin Y822 phosphorylation. The levels of phosphorylated and total vinculin in MCF10a cells induced to scatter by application of HGF for 2 h (B) or in MDCK cells overexpressing Snail (C) were examined and presented as described in A. #, $P < 0.05$; *, $P < 0.01$. (D and E) Localization of phospho-Y822 in cells; MCF10a vinculin knockdown cells rescued with GFP-vinculin (E) or MCF10a parental cells (D) were examined by immunofluorescence with affinity-purified phosphospecific antibodies against Y822 (D and E) and E-cadherin or talin (D). The phospho-Y822 antibodies specifically stain adherens junctions but not focal adhesions. Bars, 20 µm. Images are representative of three independent experiments. Average Pearson correlation coefficient reported from three independent experiments ± SEM.

Notwithstanding the similarity and interdependency, the behavior of cell–cell and cell–matrix adhesions is often discrete and unrelated, suggesting that distinct regulatory mechanisms exist for regulating force transmission. In this study, we examine how force transmission by integrins and cadherins can be differentially regulated. We focused our attention on vinculin, a known shared scaffolding component of both adhesions. Not only does vinculin accumulate at both integrin- and cadherin-containing adhesions in response to force (Riveline et al., 2001; Galbraith et al., 2002; le Duc et al., 2010; Huveneers et al., 2012), but also it bears the force and transmits it to the cytoskeleton, thereby allowing cell shape to be maintained (Grashoff et al., 2010). Critical to force transmission is the interaction of the vinculin tail domain with actin (Grashoff et al., 2010). In the absence of vinculin or its binding to actin, cells are less stiff, exert lower traction forces, and are unable to remodel the cytoskeleton (Alenghat et al., 2000; Mierke et al., 2008; le Duc et al., 2010; Huveneers et al., 2012).

Here, we have identified an unexpected regulatory mechanism in which mechanical tension on cadherins, but not integrins, induces the vinculin tyrosine phosphorylation at Y822. This phosphorylation event allows for vinculin binding to β-catenin and for cell stiffening. We identify Abelson (Abl) tyrosine kinase as being activated in response to force on E-cadherin, but not integrins, and find that it phosphorylates vinculin at Y822. Finally we show that Abl inhibition prevents vinculin actions in cadherin-containing complexes, resulting in defects in cell stiffening. This work provides a novel mechanism describing how vinculin differentially supports mechanotransduction at cell–cell and cell–matrix adhesions. This work provides a paradigm for how a shared component of adhesion complexes can produce biologically distinct functions and establishes a foundation for understanding how force transmission is modulated during normal and diseased states.

Results

Vinculin is recruited to both cadherins and integrins in response to external forces. All the available information to date suggests that vinculin's role in transmitting force by integrins and cadherins is overlapping (Grashoff et al., 2010; Pasapera et al., 2010; Sumida et al., 2011; Borghi et al., 2012; Huveneers and de Rooij, 2013). However, the behavior of these adhesions is often distinct and unrelated, suggesting that mechanisms exist for vinculin to achieve site-specific functions. The focus of this study is to identify how vinculin functions can be differentially regulated in cell–cell and cell–matrix adhesions. Clues to how the site-specific functions of vinculin might be achieved arose from our early studies blotting lysates of cells cultured under different conditions with antibodies that specifically recognized vinculin tyrosine phosphorylated at Y822. During the course of these studies, we consistently noticed that epithelial cells cultured to confluence had a fourfold higher level of vinculin phosphorylated at Y822 than the same cells cultured at subconfluency (Fig. 1 A). Evidence that the phospho-Y822 antibody was specific for phosphorylated vinculin came from blotting lysates with elevated levels of tyrosine-phosphorylated proteins, where the antibody recognized a single band co-migrating with vinculin (Fig. S1 A); additionally, mutation of Y822F prevents this band from being recognized (Fig. S1 B). Similar specificity for tyrosine-phosphorylated protein was observed when vinculin was immunoprecipitated from cell lysates and immunoblotted with the phospho-Y822 antibody (Fig. S1 C).

Our data with subconfluent and confluent epithelial cells suggested that vinculin could only be phosphorylated at Y822 in epithelial cells when they were in contact with each other. We tested if disrupting the epithelial monolayer by stimulating cells to undergo an epithelial-to-mesenchymal transition would produce a loss in vinculin Y822 phosphorylation. When confluent cells were serum starved and incubated with HGF for 2 h, the cells scattered (unpublished data) and vinculin phosphorylation at Y822 dramatically and significantly decreased (Fig. 1 B). Similar decreases in vinculin phosphorylation were observed when confluent cultures of MDCK cells were induced to undergo an epithelial-to-mesenchymal transition by overexpression of the transcription factor, Snail (Fig. 1 C). These observations suggested that epithelial cells with intact cell–cell junctions have elevated tyrosine phosphorylation of vinculin. We tested whether or not these effects resulted from specific enrichment of phospho-Y822 vinculin in adherens junctions compared with focal adhesions. For these studies, the phospho-Y822 antibody was affinity purified and used to stain cells. We found that phospho-Y822 vinculin colocalized with E-cadherin with a Pearson's coefficient of $r = 0.89 \pm 0.01$ (Fig. 1 D) and a Pearson's coefficient of $r = 0.81 \pm 0.03$ for GFP-vinculin (Fig. 1 E) in adherens junctions, but not with talin ($r = 0.20 \pm 0.03$; Fig. 1 D) or GFP-vinculin ($r = 0.26 \pm 0.05$; Fig. 1 E) in focal adhesions. Hence, the phosphorylation of vinculin on Y822 is restricted to cell–cell adhesions.

We hypothesized that if vinculin was specifically phosphorylated in cell–cell junctions that stimuli which trigger the assembly of cell–cell, but not cell–matrix, adhesions might increase vinculin phosphorylation. To examine phosphorylation in response to the assembly of cell–cell adhesions, we manipulated cadherin-mediated junction formation by varying the level of extracellular calcium in the culture medium. Under conditions of low calcium, cadherin function is blocked, and epithelial cells fail to develop cell–cell junctions (Volberg et al., 1986). Restoration of calcium stimulates the rapid reformation of these adhesions (Fig. S2 A). Vinculin phosphorylation at Y822 was not detected in the absence of intact junctions (Fig. 2 A and Fig. S2 B). Phosphorylation at Y822 was elevated as early as 2 min after initiating the assembly of adherens junctions and remained elevated for 20 min. At 40 min after calcium readdition, phosphorylation at Y822 began to decrease (Fig. 2 A and Fig. S2 B). This calcium switch approach does not differentiate whether phosphorylation occurred directly via cadherins or indirectly as a result of adherens junction formation. To distinguish between these possibilities, we examined cadherin engagement in the absence of cell–cell adhesion by plating cells on surfaces coated with cadherin extracellular domains. We found that cells plated on cadherin extracellular domains for 10 or 30 min had robust levels of vinculin phosphorylation at Y822 (Fig. 2 B). When similar experiments were performed by plating cells on surfaces coated with fibronectin (an integrin ligand),

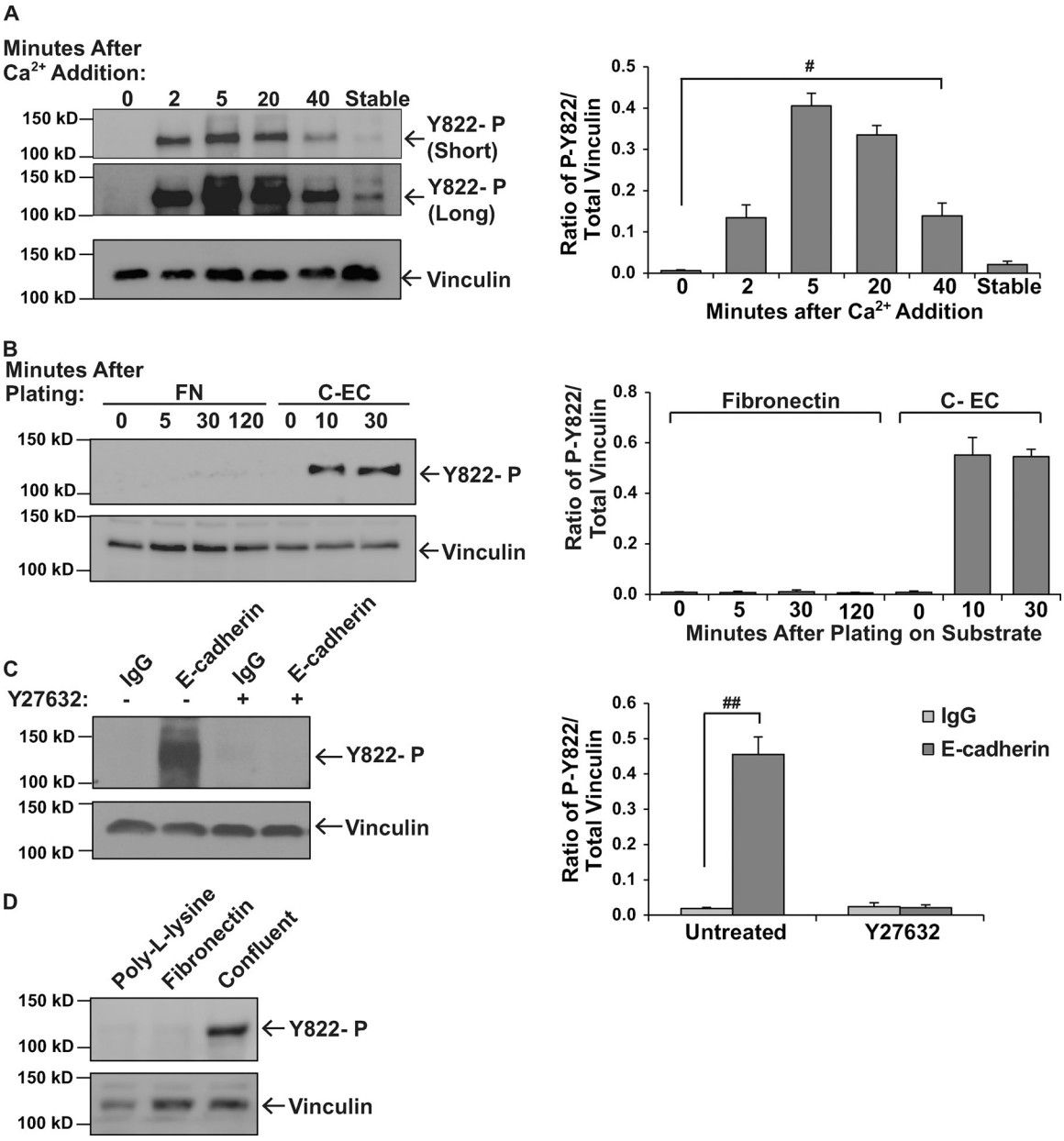

Figure 2. **Vinculin Y822 phosphorylation increases in response to engagement of and force on cadherins, but not integrins.** (A) Examination of vinculin phosphorylation during the assembly of cell–cell junctions. Cell–cell junctions were manipulated using a calcium switch procedure as described in the Materials and methods. At the indicated times after calcium restoration, cells were lysed and phospho-vinculin levels were examined, quantitated, and presented as described in Fig. 1 A. "Short" denotes short exposure of the immunoblot; "Long" denotes long exposure of immunoblot. #, $P < 0.05$. (B) The effect that integrin- and cadherin-mediated adhesion have on phospho-Y822 levels. MCF10a cells were plated on tissue culture dishes coated with cadherin extracellular domains (CEC) or human fibronectin (FN). At the specified times, cells were lysed and assayed for the levels of phosphorylated vinculin as described above. (C and D) The effect that force on cadherins or integrins has on phosphorylated vinculin. MCF10a cells were incubated with beads coated with IgG or antibodies against E-cadherin (C) or with the integrin ligand, fibronectin, or poly-lysine as a control (D), and stimulated with tensional force using a permanent magnet. The levels of phosphorylated vinculin were assessed as described above. Y-27632 indicates cells that were incubated with a ROCK1/2 inhibitor before the application of force. Results represent the means from three independent experiments. ##, $P < 0.005$.

no increases in phosphorylation were observed during the first two hours of plating (Fig. 2 B). These results suggest that cadherin- but not integrin-mediated adhesion stimulates vinculin phosphorylation.

In addition to mediating cell–cell adhesion, both cadherins and integrins sense extracellular forces and transduce this information to the cell interior via recruitment of vinculin (Riveline et al., 2001; Galbraith et al., 2002; le Duc et al., 2010; Huveneers et al., 2012). We tested whether or not application of force on E-cadherin or integrins increased vinculin phosphorylation. For this, we coated magnetic beads with antibodies against E-cadherin or an integrin ligand (fibronectin) and permitted the beads to adhere to MCF10a cells; a constant force was then applied to the beads using a permanent ceramic magnet (Guilluy et al., 2011). We found that when force was applied to beads coated with antibodies against E-cadherin that phosphorylation was robustly increased (Fig. 2 C) and could be blocked by pre-incubation of the cells with the Rho kinase inhibitor,

Y27632. Tyrosine phosphorylation was also inhibited by preincubation with 25 µM blebbistatin (Fig. S2 C). Application of force on integrins did not increase vinculin phosphorylation (Fig. 2 D).

Our data indicated a critical role for vinculin phosphorylation at Y822 in establishing and maintaining cadherin-mediated adhesion. To test this possibility directly, we generated a mutant version of vinculin that harbors an Y822F substitution and consequently cannot be phosphorylated at this site. We expressed this mutant version of vinculin in MCF10a cells that have a 90% knockdown of endogenous vinculin, which we and others have shown results in a preferential depletion of vinculin from adherens junctions (Maddugoda et al., 2007; Peng et al., 2010). Previous studies suggested that vinculin-null F9 cells re-expressing Y822F vinculin were resistant to apoptosis as a consequence of enhanced binding of paxillin and its binding partner FAK, culminating in elevations in ERK activity (Subauste et al., 2004). However, we consistently did not observe any differences in the amount of paxillin bound to FAK from cells expressing Y822F or wild type (WT; Fig. S3). We then began to examine adherens junctions in the knockdown cells rescued with Y822F vinculin. As a first measure of adherens junction integrity, we examined the morphology of the cells when plated at confluence. Phase-contrast images of cells expressing Y822F vinculin showed that the epithelial cell morphology was altered compared with cells rescued with wild-type vinculin (Fig. S4 A). Specifically, Y822F rescue cells resembled cells lacking vinculin in that they lost their honeycomb shape that is characteristic of control epithelial cells. To determine whether the phenotypic changes in the Y822F-expressing cells were the result of a loss of adherens junctions, we examined the integrity of the cell–cell junctions using transmission EM. Electron micrographs showed that the Y822F rescue cells failed to make cohesive contact with adjacent cells, whereas control and WT rescue cells formed adherens junctions in the regions between neighboring cells (Fig. S4 B). To determine if the morphological changes were due to an effect on E-cadherin, immunofluorescence was used to examine the localization of E-cadherin in confluent cell monolayers. Both the vinculin knockdown cells and the Y822F rescue cells had reduced levels of E-cadherin staining at cell–cell junctions (Fig. 3 A). Additionally, Y822F failed to localize to adherens junctions (Fig. 3 A). Re-expression of wild-type vinculin restored E-cadherin staining at the junctions. To determine whether the morphological differences that we observed in the Y822F rescue cells were due to a loss of cadherin-mediated adhesion, we measured the ability of the cells to bind to the extracellular domains of cadherin proteins. Unlike the control and wild-type rescue cells, which adhered to the cadherin extracellular domains, the Y822F rescue cells were significantly impaired in adhesion to an extent that was similar to the knockdown cells (Fig. 3 B). Moreover, these differences were not attributed to the levels of re-expression, as both the wild-type and Y822F rescue cells had similar levels of re-expression (Fig. S4 C). They also were not attributed to differences in the levels of E-cadherin expression (Fig. S4 D).

To investigate force transduction downstream of E-cadherin in vinculin knockdown cells rescued with Y822F, we applied tensional forces (using three-dimensional force microscopy [3DFM]) to paramagnetic beads coated with antibodies or ligands to endogenous proteins. Using this approach, pulses of force are applied on the bead and the cells respond by increasingly resisting bead displacement. When pulses of force were applied to endogenous E-cadherin in the WT rescue cells, a significant decrease in pulse-to-pulse bead displacement was observed, indicative of force-dependent adaptive stiffening, (Fig. 3 C). In contrast, when force was applied to E-cadherin in the Y822F rescue cells, there was a lack of reinforcement in response to pulses of force (Fig. 3 C). To examine vinculin phosphorylation in response to tensional forces on E-cadherin, magnetic beads bound to E-cadherin in the WT rescue cells were subjected to force using a permanent ceramic magnet. Force application increased vinculin phosphorylation at Y822; this increase was blocked by the Y822F mutation (Fig. 3 D). These findings indicate that vinculin becomes phosphorylated on Y822 in response to force transmission by cadherins but not integrins.

We next explored why Y822F could not support cadherin functions. We tested if Y822F could bind β-catenin, one of the proteins that is necessary for vinculin concentration in the cadherin adhesion complex (Hazan et al., 1997; Peng et al., 2010). We found that wild-type vinculin bound β-catenin quite well, whereas Y822F did not (Fig. 3 E). Taken together, these findings suggest that Y822F vinculin does not support cadherin-mediated force transmission or adhesion as a consequence of its inability to bind β-catenin and integrate into the cadherin adhesion complex.

We examined if Y822F could support integrin-mediated adhesive events. As a first measure, the morphology of subconfluent cells plated on fibronectin was examined. We did not note any gross morphological differences between MCF10a knockdown cells rescued with wild-type or Y822F vinculin when plated at low density, but noted that in some instances the cells appeared more spread (Fig. 4, A and D). Like WT vinculin, Y822F vinculin was enriched in paxillin-containing focal adhesions in epithelial cells (Fig. 4 B) and precipitated a similar amount of talin (Fig. 4 C). Because we observed some slight changes in morphology at low magnification, we examined integrin-mediated events in the MCF10a vinculin knockdown cells rescued with wild-type or Y822F vinculin. The Y822F rescue cells adhered, spread, and migrated better than those cells rescued with wild-type vinculin (Fig. 4 D). Interestingly, Y822F supported integrin-mediated adhesive events to a statistically higher extent than the wild-type rescue cells. All of the studies described thus far were performed in epithelial cells. We tested if Y822F was also able to rescue integrin-mediated events to a greater extent in mouse embryo fibroblasts isolated from the vinculin-null mouse (Fig. 4, E and F). Y822F colocalized with paxillin in these cells (Fig. 4 E), and we noted more focal adhesions and a greater level of cell spreading (Fig. 4 F) in the Y822F rescue cells when compared with the WT rescue cells.

In addition to being required for integrin-mediated adhesion, vinculin is critical for force transmission by integrins. Consequently, we tested if Y822F could support integrin-mediated force transduction. When we applied tensile forces (using 3DFM) to paramagnetic beads coated with fibronectin on the WT or

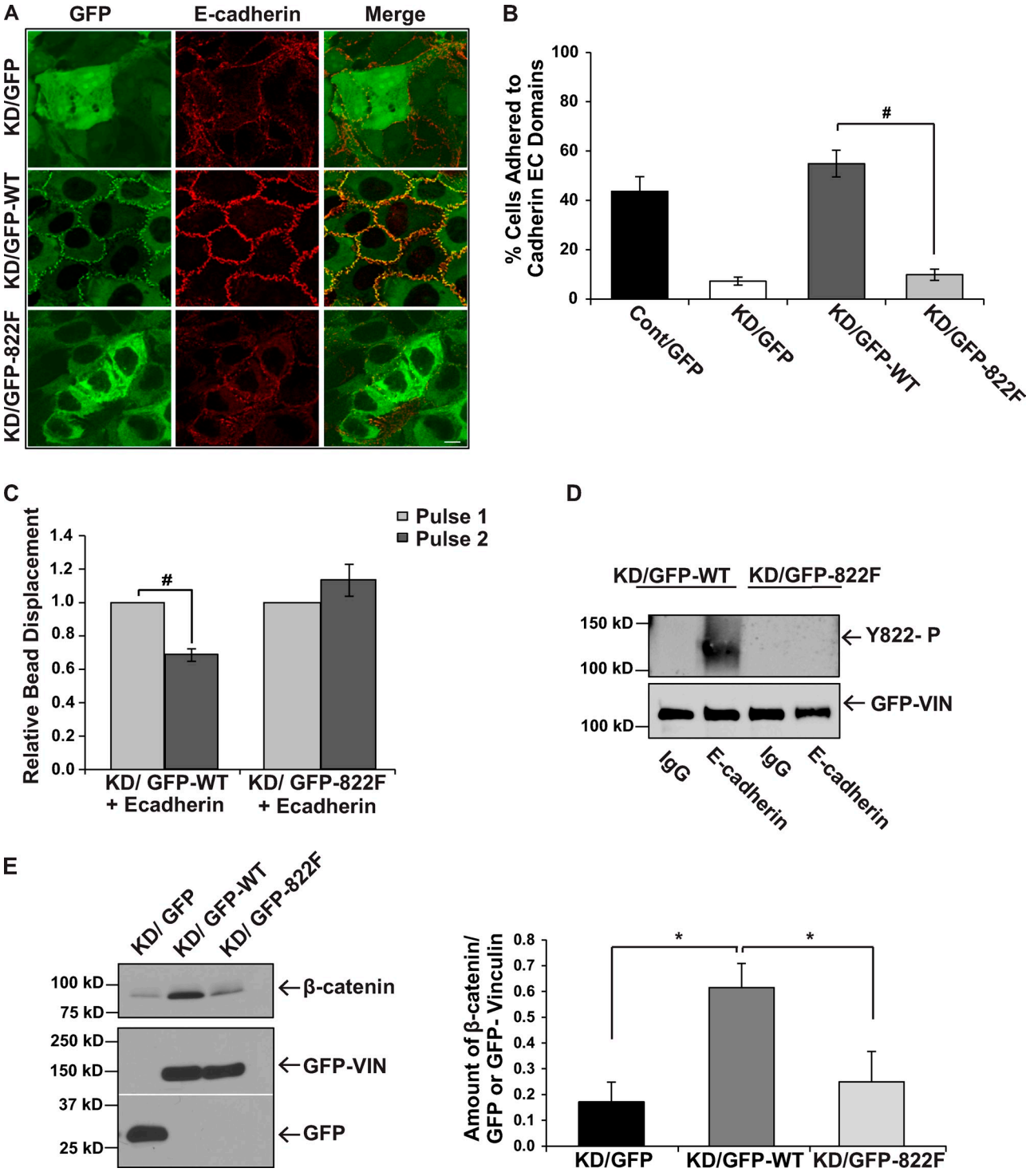

Figure 3. **Y822F vinculin does not support cadherin-mediated adhesion or force transmission.** MCF10a cells were infected with GFP, GFP-tagged chick vinculin (GFP-WT), or a mutant version of vinculin with a Y822F substitution (GFP-822F), and then infected a second time with either an empty vector (Cont) or an shRNA vector targeting human vinculin (KD). (A) Examination of E-cadherin localization by immunofluorescence. The Y822F mutant vinculin does not rescue E-cadherin localization to adherens junctions in cells with low levels of vinculin. Bar, 10 µm. (B) Examination of the adhesion of the indicated cells to cadherin extracellular (EC) domains. For assessing homophilic ligation, cells were plated on dishes coated with human E-cadherin extracellular domains fused to Fc, and were washed. The percentages of cells that adhered (±SEM from three independent experiments) are shown. #, $P \leq 0.05$. (C) Pulses of force were applied to magnetic beads coated with Fc-tagged E-cadherin that have been incubated on MCF10a knockdown cells rescued with either GFP-WT or GFP-Y822F vinculin. Experiments are the relative means ± SEM and have been normalized to the first pulse. WT vinculin + E-cadherin beads (n = 30); Y822F vinculin + E-cadherin beads (n = 30). Statistical significance was determined by two-tailed Student's t test. #, $P \leq 0.05$. (D) The effect of Y822F substitution on E-cadherin induced vinculin Y822 phosphorylation in response to force. Force was exerted on magnetic beads as described in the legend of Fig. 2 C and vinculin phosphorylation was measured and depicted as described in Fig. 1 A. Results are representative of three independent experiments. (E) The levels of β-catenin that coimmunoprecipitated with GFP, GFP-WT vinculin, or GFP-Y822F vinculin were assessed using immunoblotting. The left panel shows representative immunoblots and the right panel is a quantification of the average amount of bound protein normalized for the amount of GFP protein recovered in three independent experiments. β-Catenin bound GFP-Y822F at reduced levels compared with WT vinculin. *, $P \leq 0.01$.

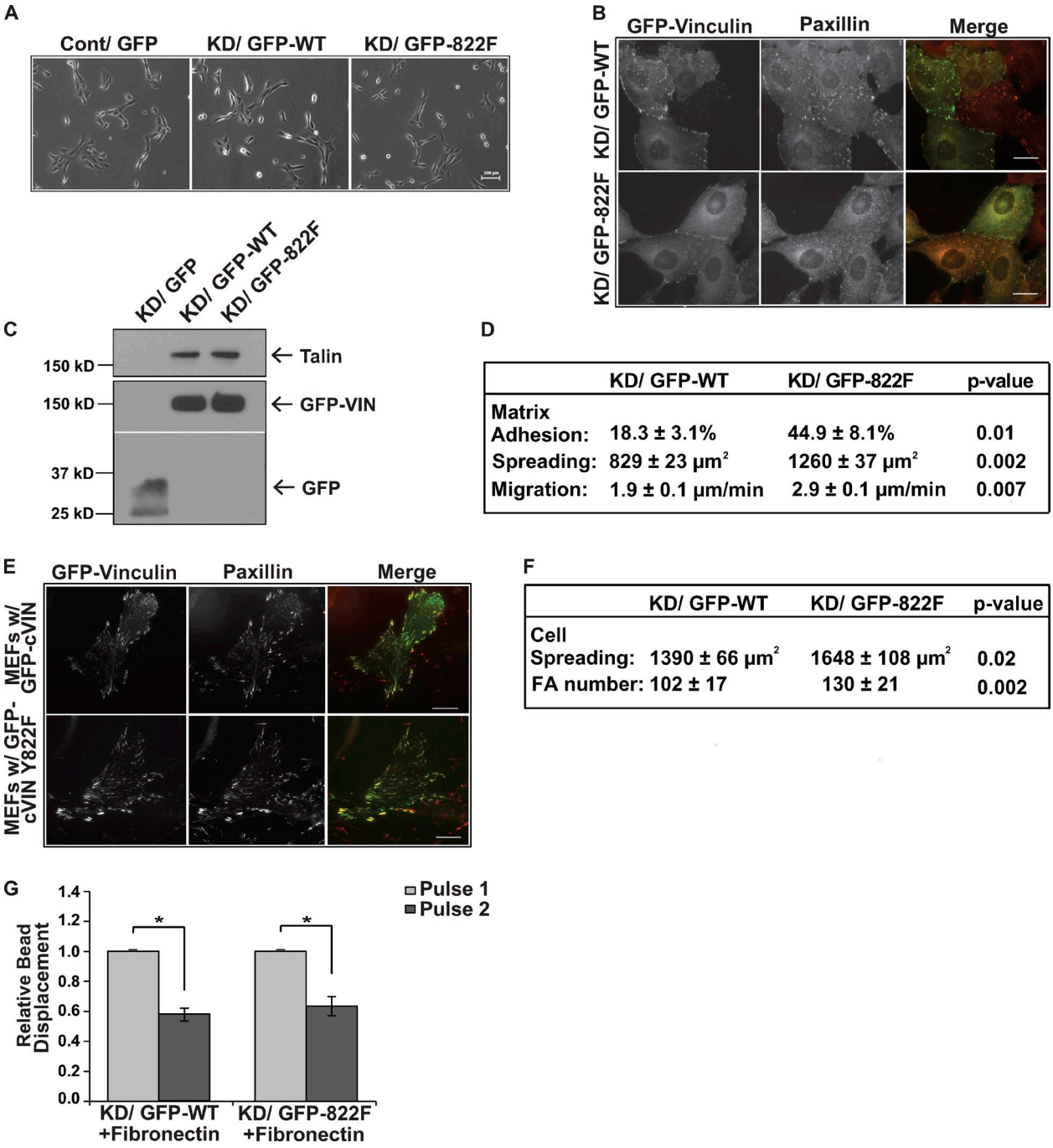

	KD/ GFP-WT	KD/ GFP-822F	p-value
Matrix Adhesion:	18.3 ± 3.1%	44.9 ± 8.1%	0.01
Spreading:	829 ± 23 μm^2	1260 ± 37 μm^2	0.002
Migration:	1.9 ± 0.1 μm/min	2.9 ± 0.1 μm/min	0.007

	KD/ GFP-WT	KD/ GFP-822F	p-value
Cell Spreading:	1390 ± 66 μm^2	1648 ± 108 μm^2	0.02
FA number:	102 ± 17	130 ± 21	0.002

Figure 4. **Blocking vinculin phosphorylation at Y822 does not inhibit integrin adhesion, force transmission, or talin recruitment.** (A–D) Examination of the ability of Y822F to support integrin-mediated adhesion and force transmission in epithelial cells. (A) Subconfluent cultures of vinculin knockdown MCF10a cells rescued with GFP-vinculin (KD-GFP-WT) or Y822F vinculin (KD/GFP-822F) or control MCF10a cells expressing GFP (Cont/GFP) were examined by phase-contrast microscopy. No differences were observed in cell morphology. Bar, 100 μm. (B) Examination of Y822F localization in focal adhesions. The cells were stained with antibodies against paxillin. GFP-WT and GFP-Y822F vinculin localized to focal adhesions to similar extents. Bars, 20 μm. (C) The levels of talin that coimmunoprecipitated with GFP, GFP-WT vinculin, or GFP-Y822F vinculin were assessed using immunoblotting. Unlike β-catenin, talin bound GFP-Y822F to wild-type levels. (D) Summary of the ability of Y822F vinculin to support integrin-mediated events. Matrix adhesion indicates the percentage of cells that adhered to 10 μg/ml fibronectin. Cell spreading indicates the area of cells (as measured using ImageJ) that were allowed to spread on 10 μg/ml of fibronectin for 4 h. Cell migration indicates the cell speed of individual cells randomly migrating on fibronectin. The average cell speed (±SEM) was calculated from three independent experiments. (E and F) An examination of the ability of Y822F to support integrin-mediated events in mouse embryo fibroblasts isolated from the vinculin-null mouse. (E) Colocalization of GFP-WT or GFP-Y822F vinculin with paxillin as examined by immunofluorescence. Bars, 20 μm. (F) The ability of the WT and Y822F cells to spread on fibronectin-coated surfaces was examined as described in D; the average number of focal adhesions per cell were counted and expressed as the average ± SD. Cells expressing Y822F spread slightly better and had slightly more focal adhesions than those expressing WT vinculin. (G) Pulses of force were applied to fibronectin-coated magnetic beads that were incubated on MCF10a knockdown cells rescued with either GFP-WT or GFP-Y822F vinculin. Experiments are the relative means ± SEM and have been normalized to the first pulse. WT vinculin + fibronectin beads (n = 19); Y822F vinculin + fibronectin beads (n = 20). Statistical significance was determined by two-tailed Student's t test; *, $P \leq 0.01$.

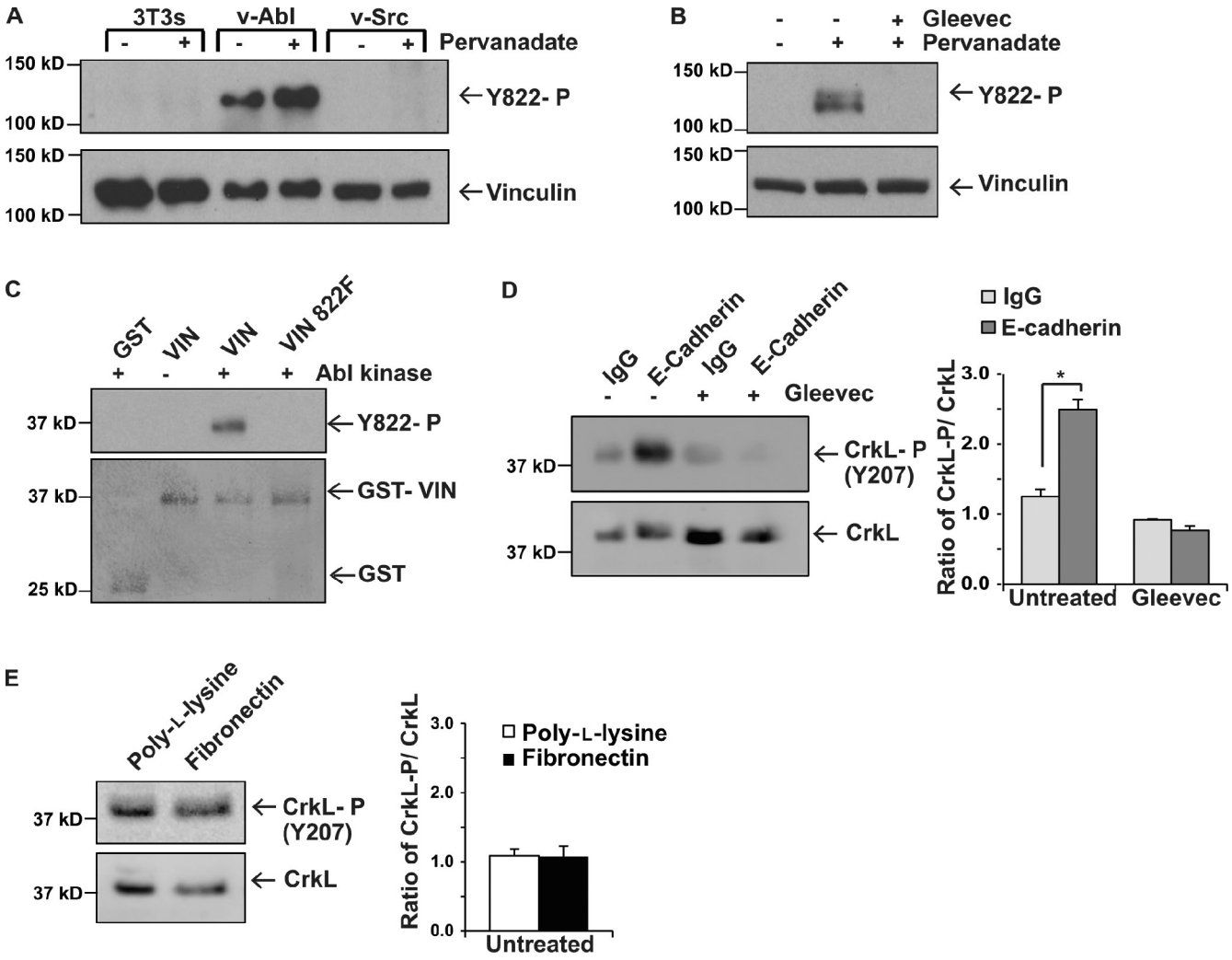

Figure 5. **Abl is the tyrosine kinase that phosphorylates vinculin Y822.** (A and B) Examination of vinculin phosphorylation on Y822 as described in Fig. 1 A. (A) NIH3T3 cells, NIH3T3 cells transformed with the Rous sarcoma virus (v-Src), or BALB/c fibroblasts transformed with Abelson mouse leukemia virus (v-Abl) were left resting (−) or treated with pervanadate (+) before examination of pY822 phosphorylation. (B) MCF10a parental cells were left resting or treated with the phosphatase inhibitor pervanadate; Gleevec indicates cells pretreated with this Abl inhibitor. (C) In vitro kinase assay using Abl. Purified GST or GST vinculin 811–881 proteins were incubated with recombinant Abl in the presence or absence of 5 µM Gleevec. The samples were fractionated by SDS-PAGE and the bottom portion of the gel was stained to show the amounts of protein used (bottom); the top of the gel was immunoblotted with a phospho-Y822 specific antibody. All results are representative of three independent experiments. (D and E) Effect that application of force on E-cadherin or integrins has Abl tyrosine kinase activity. Force was exerted on magnetic beads coated with antibodies against E-cadherin (D) or fibronectin (E) as described in the legend of Fig. 2 C and phosphorylation of CrkL, an Abl substrate, was examined by immunoblotting with antibodies that recognize Y207 (the Abl-specific site) or total CrkL levels (left). Quantification of the results of three independent experiments is shown in the graph in the right-hand panel. IgG and poly-L-lysine indicate the controls. *, $P < 0.01$.

Y822F rescue cells, both cell types resisted bead displacement, suggesting force-dependent adaptive stiffening (Fig. 4 G). Taken together, these data indicate that Y822F vinculin is able to integrate into the integrin adhesion complex and support integrin adhesive events and force transmission to at least wild-type levels in epithelial and fibroblast cell lines.

We sought to identify the kinase responsible for phosphorylating vinculin at Y822. Abl and Src tyrosine kinases were good candidates, as vinculin is highly phosphorylated in cells transformed by the Rous sarcoma and Abelson viruses (Sefton et al., 1981). Moreover, both Abl and Src are activated in response to cadherin engagement, and epithelial cells with Abl or Src inhibited have disruptions in junction integrity that are reminiscent of those observed in the Y822F-expressing cells (Calautti et al., 1998; Owens et al., 2000; McLachlan et al., 2007; Zandy et al., 2007; Zandy and Pendergast, 2008). We analyzed vinculin Y822 phosphorylation levels in cells overexpressing v-Abl or v-Src and treated with or without the phosphatase inhibitor pervanadate. We found that vinculin Y822 was not phosphorylated in the parental cells as would be expected for a cell line lacking adherens junctions. In contrast, Y822 was highly phosphorylated in v-Abl–overexpressing cells (Fig. 5 A). This effect was specific to cells overexpressing Abl, as vinculin was not phosphorylated in the same cells overexpressing v-Src. To determine if this phosphorylation event was limited to cells overexpressing activated forms of these kinases, we examined vinculin phosphorylation in MCF10a cells. We found that cells treated with pervanadate had elevated phospho-Y822 levels that

could be inhibited by pre-incubation of cells with Gleevec (imatinib), an Abl tyrosine kinase inhibitor (Fig. 5 B). We tested if vinculin can be phosphorylated in vitro at Y822 by recombinant Abl kinase. For these studies, the purified vinculin linker domain (residues 811–881) or a linker domain unable to be phosphorylated at Y822 (i.e., Y822F) fused to GST or GST alone were incubated with purified Abl kinase. Fig. 5 C shows that Abl directly phosphorylates vinculin Y822 but not purified GST. Furthermore, this phosphorylation did not occur when protein with the Y822F mutation was used, confirming that this is the critical site (Fig. 5 C).

Having established Abl as the kinase that phosphorylates vinculin, the critical question became whether or not Abl is activated by force on E-cadherin and if Abl inhibition produces defects that mirror Y822F vinculin. We first examined whether application of force on E-cadherin activated Abl. For this, we applied tensile forces to E-cadherin and tested whether Abl is catalytically activated by analyzing the phosphorylation of the Abl substrate CrkL using phosphospecific antibodies against the Abl-specific sites, which have been shown to be unphosphorylated in $Abl^{-/-}$ MEFs or in cells lacking Abl kinase activity (Burton et al., 2003; Zipfel et al., 2004). In response to mechanical tension on E-cadherin, Abl kinase activity was elevated 4.6-fold (Fig. 5 D), and this increase in activity could be blocked by pre-incubation of cells with Gleevec. In contrast, Abl was not activated in response to force on integrins (Fig. 5 E).

We next examined if inhibition of Abl mimicked a loss of vinculin phosphorylation at Y822. We found that pre-incubation of cells with the Abl inhibitor Gleevec completely blocked β-catenin recruitment to wild-type vinculin (Fig. 6 A) and produced disruptions in adherens junctions that were evident by immunofluorescence staining (Fig. 6 B). The magnitudes of the effects were similar to those observed in the Y822F rescue cells (compare Fig. 6, A and B with Fig. 3, A and E). Furthermore, pre-incubation of cells with Gleevec prevented cells from responding to pulses of force on E-cadherin by reinforcement (Fig. 6 C). Gleevec treatment also blocked vinculin phosphorylation in response to application of force on E-cadherin (Fig. 6 D). We also considered the consequence that Abl inhibition would have on integrin-mediated events. When we treated cells with Gleevec, we found that matrix adhesion was increased by 2.3-fold and cell spreading was increased by 1.6-fold (Fig. 6 E). This finding is in line with our observations that Y822F vinculin increases cell adhesion by 2.2-fold and cell spreading by 1.5-fold. This increase in integrin function in response to Gleevec is also consistent the observations made by other groups. Collectively, these findings indicate that Abl phosphorylates vinculin at Y822 in response to mechanical force and that inhibition of Abl kinase activity prevents vinculin adhesive and force-transducing functions in cell–cell junctions.

Discussion

Unlike many of the components of cell–cell and cell–matrix adhesions that are localized at only one adhesion site, vinculin is present in both complexes and is required for force transmission (Geiger, 1979; Geiger et al., 1980). The enrichment of vinculin in cell–cell junctions is elevated when external forces are applied (le Duc et al., 2010; Yonemura et al., 2010; Sumida et al., 2011). In the 30 years since vinculin was identified (Geiger, 1979), a satisfactory explanation for this differential distribution has not been provided. This unanswered question has resurfaced, owing to observations that vinculin is required for force transmission not only by integrins, but also cadherins (le Duc et al., 2010; Huveneers et al., 2012). Our finding that force on E-cadherin activates Abl and that Abl-mediated phosphorylation of vinculin on Y822 promotes its binding to β-catenin identifies a mechanism by which vinculin is selectively driven to adherens junctions.

The idea that vinculin phosphorylation at Y822 is a determinant for vinculin function in adherens junctions is novel. Previous reports suggested that cells expressing Y822F were resistant to apoptosis, owing to substantial elevations in Erk activity that could be accounted for by increased recruitment of paxillin to its binding partner FAK (Subauste et al., 2004). In our studies, we found that paxillin recruitment to FAK was unaffected by mutation of Y822F vinculin, arguing against a role for Y822 in mediating the apoptotic response (Fig. S3). A different previous study indicated a role for Y822F in regulating basal stiffness of teratoma cell lines (Goldmann et al., 1998). Our observation that MCF10a vinculin knockdown cells rescued with Y822F stiffen in response to force on integrins does not support a role for tyrosine phosphorylation in mediating cell stiffening. The reasons for the differences between our studies and the previous one are not yet known. One possibility is that basal cell stiffness and stiffening in response to force on integrins use different signaling events, only one of which requires vinculin Y822 phosphorylation. Alternatively, it is possible that the different cell lines have distinct requirements for stiffening.

We considered how vinculin phosphorylation at Y822 might regulate vinculin function and/or activation at sites of cell–cell and cell–matrix. We tested whether or not substitution of Y822F affected vinculin binding to actin but we consistently observed no change (Fig. S5). We also found no evidence that phosphorylation of Y822 affects recruitment of binding partners to the linker region of vinculin (unpublished data). These observations argue against phospho-Y822 regulating vinculin activation. Our observation that substitution of Y822F prevents recruitment of β-catenin (but not talin) to the vinculin head suggests that the conformation of the vinculin head domain may be changed by phosphorylation at Y822. Ongoing studies are aimed at addressing this possibility.

Our findings identify Abl as the kinase that phosphorylates Y822 and differentially regulates vinculin in cell–cell junctions and focal adhesions. Such a role for Abl in regulating cell–cell junction function is anticipated from observations that patients treated with Gleevec suffer from side effects owing to a loss of adherens junction function, including edema (Irvine and Williams, 2013), immune-mediated liver damage (Irvine and Williams, 2013), and skin rashes (Niessen, 2007; Brazzelli et al., 2013). The selectivity of Abl for vinculin in cell–cell junctions is the result of Abl being activated when force is applied to cadherins, but not integrins (Fig. 5, D and E). The engagement of both integrins and cadherins stimulates Abl activity, so it is

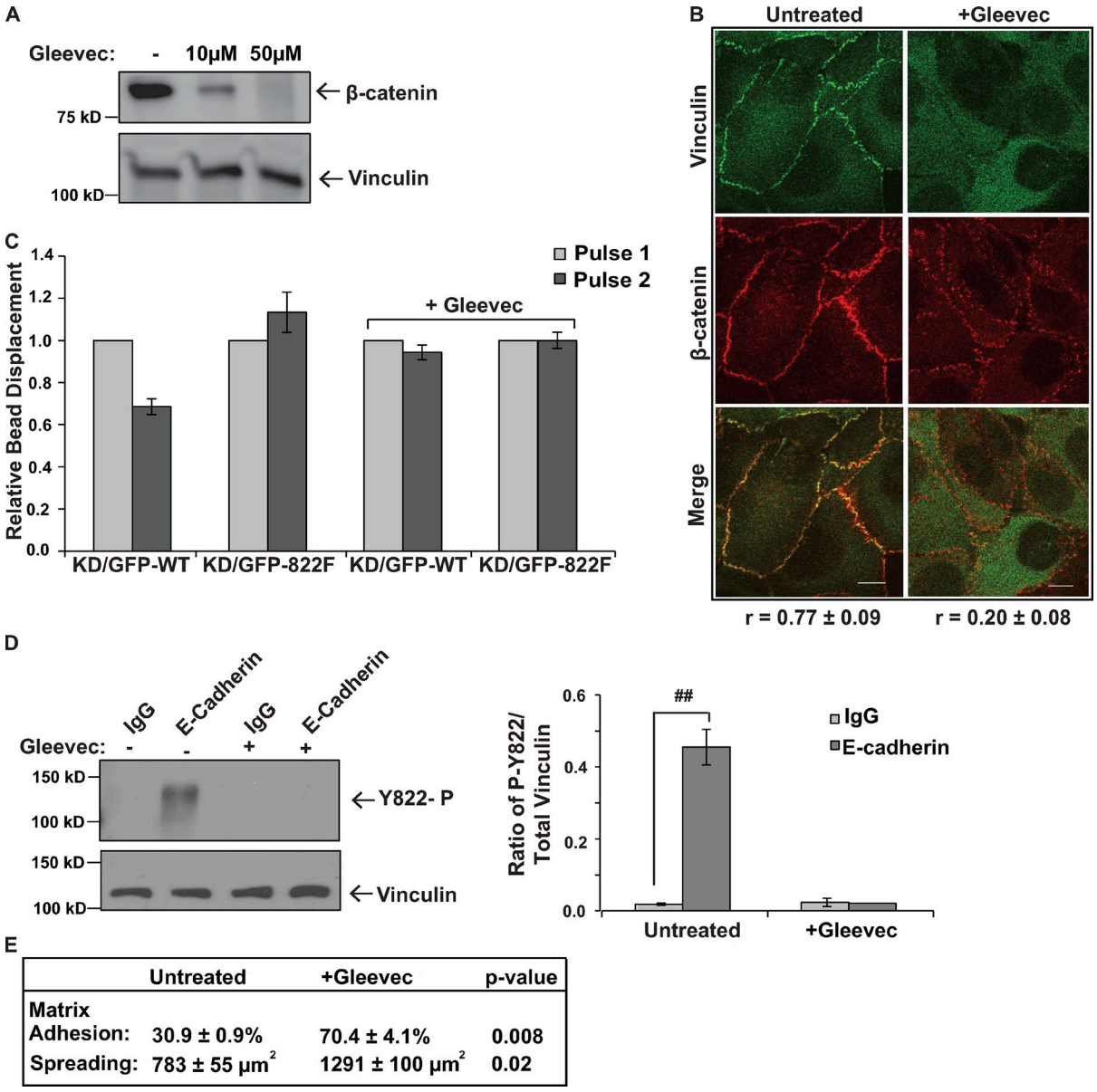

	Untreated	+Gleevec	p-value
Matrix Adhesion:	30.9 ± 0.9%	70.4 ± 4.1%	0.008
Spreading:	783 ± 55 μm^2	1291 ± 100 μm^2	0.02

Figure 6. **Inhibition of Abl mimics loss of vinculin phosphorylation at Y822.** (A and B) β-catenin recruitment to and colocalization with vinculin when Abl is inhibited. MCF10a cells were left resting (−) or treated with Gleevec. (A) Vinculin was immunoprecipitated from parental cells and the levels of bound β-catenin were examined by immunoblotting. The blot was stripped and reprobed with antibodies against vinculin to reveal the amounts of proteins recovered. (B) MCF10a vinculin knockdown cells expressing GFP-vinculin were left untreated or treated with Gleevec and then analyzed by immunofluorescence with antibodies against β-catenin. Average Pearson correlation coefficient is reported below images (±SD). Bars, 10 μm. (C) Effects of Gleevec on E-cadherin–induced cellular stiffening. MCF10a vinculin knockdown cells re-expressing WT or Y822F vinculin were incubated with magnetic beads coated with Fc-tagged E-cadherin and were treated with or without Gleevec. 3DFM was used to measure the bead displacement on individual cells. Relative bead displacement is shown. WT vinculin (n = 30); Y822F vinculin (n = 30); WT vinculin + Gleevec (n = 30); Y822F vinculin + Gleevec (n = 30). (D) MCF10a cells were incubated with magnetic beads coated with antibodies against E-cadherin or IgG in the presence (+) or absence (−) of Gleevec. Tensional force was generated on the beads using a permanent magnet and phospho-Y822 or total vinculin levels were examined as described in Fig. 1 A. All results are representative of at least three independent experiments. ##, $P < 0.005$. (E) Effects of Gleevec on cell–matrix events. The ability of the GFP-WT cells to adhere to or spread on fibronectin-coated surfaces was examined as described in Fig. 4 D after 2 h of treatment with 20 μM Gleevec and expressed as averages ± SEM.

striking that only application of force to cadherins activates Abl (Kain and Klemke, 2001; Zandy et al., 2007; Zandy and Pendergast, 2008). This finding is in line with previous reports showing that force on integrins activates RhoA (Guilluy et al., 2011), and Abl family kinases negatively regulate RhoA through activation of p190RhoGAP (Bradley et al., 2006; Chen et al., 2013). Hence, multiple studies support the idea that Abl is not activated when forces are applied to integrins.

We consistently noted that when cells were rescued with Y822F vinculin or treated with Gleevec that they were better able to execute integrin-mediated events than their wild-type counterparts (Fig. 5 and Fig. 6 E); this difference was not attributable to higher expression levels of Y822F vinculin (Fig. 3 E). It is also unlikely that this difference can be accounted for by more Y822F vinculin in a focal adhesion when it is lost from cell–cell junctions, as there is a vast excess of vinculin in a cell.

An alternative possibility is that the integrin-mediated events are up-regulated because cadherins are no longer present to antagonize the effects of integrins. However, we observed that Y822F is better able to up-regulate integrin-mediated events in mouse embryo fibroblasts that lack epithelial cell–cell junctions (Fig. 5), suggesting that additional pressures exist. Previous studies with other mutant vinculins show that there is an accumulation of focal adhesions when protein turnover is altered (Saunders et al., 2006). When we expressed Y822F in the vinculin-null mouse embryo fibroblasts, we found that there were more focal adhesions than in cells expressing wild-type vinculin (Fig. 4). Hence, it may be that the increase in the magnitude of the effect with Y822F can be attributed to altered focal adhesion dynamics.

In summary, it has never really been answered how the functions of vinculin at one adhesion complex can be differentiated from others. Our data reveal that the ability of vinculin to be phosphorylated at Y822 determines whether cadherins or integrins transmit force. This new information provides insight into how shared components of force-transducing machineries can be differentially regulated and establishes a foundation for understanding how force transmission is modulated during histogenesis, morphogenesis, and tumorigenesis.

Materials and methods

Constructs

Endogenous vinculin was silenced using pSUPER-shVIN that was generated by subcloning an oligo targeting the human vinculin sequence TTCAAGAGA into the retroviral vector pSUPER-RETRO-PURO (Oligoengine; Peng et al., 2010). pLEGFP-WT vinculin was generated by amplifying full-length chicken vinculin, ligating it into the pENTR-DTOPO and then cloning it into a pLEGFP-DEST vector using the Gateway cloning system (Invitrogen). pLEGFP-DEST was digested with HindIII and BamH1 and ligated into pLEGFP-C1 vector and expression driven by CMV promoter. pLEGFP-vinculin Y822F was prepared using site-specific mutagenesis to introduce the appropriate single amino acid substitution into pLEGFP-WT vinculin (Peng et al., 2010). Full-length Snail was cloned into the pQCXIP retroviral vector and expression driven by CMV promoter (Place et al., 2013). pGEX4T1-vinculin 811–881 were constructed by PCR amplifying corresponding residues of chick vinculin and subcloning this into pGEX4T1 (GE Healthcare). pGEX4T1-vinculin 811–881 Y822F were prepared by using site-specific mutagenesis to introduce a mutation resulting in the appropriate single amino acid substitution into pGEX4T1-vinculin 811–881.

Cell lines

MCF10a human breast epithelial cells (American Type Culture Collection) were maintained in DMEM/F12 (1:1) medium supplemented with 5% horse serum, 500 units each of penicillin/streptomycin, 20 ng/ml EGF, 0.5 mg/ml hydrocortisone, 100 ng/ml cholera toxin, and 10 µg/ml insulin. 293GPG cells are a virus-producing cell line and are a derivative of 293T cells, and were maintained in DMEM medium supplemented with 10% heat-inactivated FBS, 500 units each of penicillin/streptomycin, 2 mM L-glutamine, 1 µg/ml tetracycline, 2 µg/ml puromycin, 0.5 mg/ml G418, and 20 mM Hepes. During retrovirus production, 293GPG cells were maintained in virus-producing medium (DMEM supplemented with 10% heat-inactivated FBS, 500 units each of penicillin/streptomycin, 2 mM L-glutamine, and 20 mM Hepes). Vinculin-null mouse embryo fibroblasts were the gift of Eileen Adamson (Burnham Institute, La Jolla, CA) and were characterized by Xu et al. (1998). MDCK cells overexpressing pQCXIP or pQCXIP Snail were the gift of Trent Place and Frederick Domann (University of Iowa, Iowa City, IA) and were maintained in DMEM supplemented with 10% heat-inactivated FBS and 500 units each of penicillin/streptomycin (Place et al., 2013). The cells expressing v-Src were derived from BALB/c mice transformed with Rous sarcoma virus. Cells overexpressing v-Abl were derived from BALB/c mice transformed with Abelson mouse leukemia virus and obtained from American Type Culture Collection.

Adhesion assays

Cadherin extracellular domains were isolated from media collected from CHO cells with pEE14 construct encoding the truncated cadherin lacking the cytoplasmic tail by passing media over a protein G column and eluting with 0.1 M glycine, pH 2.5, and 1 mM Ca^{2+} into tubes containing 1 M Tris, pH 8.8 (Peng et al., 2010). Fibronectin was isolated by passing human plasma over Sepharose 4B and gelatin–Sepharose 4B columns and eluting with 4 M urea, 0.15 M NaCl, 2 mM EDTA, 2 mM PMSF, and 20 mM Tris, pH 7.6 (Ruoslahti et al., 1982). Tissue culture dishes were coated with 2 µg/ml of cadherin extracellular domain or 10 µg/ml of fibronectin at 4°C overnight, and then were washed two times with PBS (fibronectin) or Hepes-buffered saline with calcium (cadherin extracellular domains). The fibronectin-coated surfaces were blocked with 10 mg/ml BSA in PBS for 1.5 h at 37°C and washed two times with serum-free DMEM. MCF10a cells were lifted in 3 mM EDTA in PBS at 37°C, washed in serum-free DMEM, counted, and then plated on surfaces coated with fibronectin and incubated at 37°C for 4 h or the indicated times. The cells were then washed gently 2× with PBS or HBSC and fixed in 3.7% formaldehyde in PBS for 10 min. The numbers of cells adhered per 10 fields of view were counted, averaged, and then used to calculate the percentage of cells that adhered.

Cell spreading

Cells were plated on 10 µg/ml fibronectin-coated plates for 4 h, fixed in 3.7% formaldehyde in PBS for 10 min, and imaged using an inverted light microscope (Axiovert 200M; Carl Zeiss). Cell area was calculated using ImageJ software (National Institutes of Health).

Migration studies

MCF10a cells were plated for ∼18–24 h. The cells were then imaged using an inverted light microscope (Axiovert 200M; Carl Zeiss) and imaged using an ORCA-ER camera (Hamamatsu Photonics) using Axiovision software (Carl Zeiss) in a heated (37°C) and humidified chamber (5% CO_2). The cells were allowed to randomly migrate for 18 h, with the imaging software taking a picture of the cells every 10 min. ImageJ software was used to track the progression of the cells throughout the frames and calculate the motility rates of multiple cells for each cell line.

Cell stimulation

For HGF treatment, cells were serum starved in serum-free media for 4–5 h and then treated with recombinant human HGF (PeproTech) at 30 ng/ml for 2 h at 37°C. The calcium-switch assays were performed by incubating cells in calcium-free media for 12 h and then restoring calcium-containing media for the times indicated. Pervanadate solution was prepared by mixing equal volumes of 20 mM H_2O_2 and 200 mM Na_3VO_4. The resulting solution was added to intact cells to a final concentration of 1 mM H_2O_2 and 100 mM Na_3VO_4 for the indicated times.

Immunoprecipitation and Western blotting

Cells were washed twice in HS buffer (20 mM Hepes, pH 7.4, and 150 mM NaCl) and lysed in ice-cold EB buffer (1% Triton X-100, 10 mM Tris-HCl, pH 7.4, 5 mM EDTA, 50 mM NaCl, 50 mM NaF, 0.1% BSA, 20 µg/ml aprotinin, 2 mM Na_3VO_4, and 1 mM PMSF) or GFP immunoprecipitation buffer (50 mM Tris-HCl, pH 7.6, 150 mM NaCl, 1% NP-40, 0.5% deoxycholate, 20 µg/ml aprotinin, 2 mM Na_3VO_4, and 1 mM PMSF). GFP was immunoprecipitated with a monoclonal GFP antibody (Roche), vinculin was immunoprecipitated with a monoclonal vinculin antibody (hVIN-1; Sigma-Aldrich), and the immunoprecipitates were washed 4× in immunoprecipitation buffer, fractionated by SDS-PAGE, transferred to PVDF, blocked in 5% milk or 1% BSA (anti-phosphoY822 vinculin), and subjected to Western blot analysis. For the analysis of vinculin levels in the different shRNA knockdown cells, lysate aliquots with equal amounts of total protein (as measured using the Coomassie protein assay reagent [Thermo Fisher Scientific]) were separated on an SDS-PAGE gel. Western blotting was then performed with the appropriate antibody: vinculin was recognized using a rabbit antibody raised against purified chick gizzard vinculin (DeMali et al., 2002). The p34-Arc subunit of the Arp2/3 complex was recognized using a rabbit polyclonal antibody raised against a peptide that encompassed aa 179–204 of p34-Arc (DeMali et al., 2002). α-Catenin was recognized with a rabbit polyclonal antibody raised against human/mouse α-catenin aa 890–901 (Sigma-Aldrich); β-catenin was recognized with a rabbit polyclonal antibody raised against human/mouse β-catenin aa 768–781 (Sigma-Aldrich). Talin was recognized with a mouse monoclonal antibody that recognizes an epitope in the intact molecule (225 kD) and 190-kD fragment (Sigma-Aldrich). E-cadherin was recognized with an HECD-1 mouse monoclonal antibody (EMD Millipore). GFP was recognized with a mouse monoclonal antibody (Roche). Phosphorylated vinculin

at Y822 was recognized with a rabbit polyclonal antibody (Abcam). CrkL was recognized with a polyclonal antibody raised against the C terminus of human CrkL (C-20; Santa Cruz Biotechnology, Inc.) and phospho-CrkL was blotted with a polyclonal antibody that recognizes CrkL phosphorylated at Y207 (Cell Signaling Technology). The blots were developed using ECL Western blot detection reagents (Thermo Fisher Scientific), and the signal was detected on x-ray film (Kodak) or with a digital imaging system (ImageQuant LAS 400; GE Healthcare).

Immunofluorescence and transmission electron microscopy

Cells were fixed in 3.7% formaldehyde in phosphate-buffered saline (PBS), permeabilized in 0.5% Triton X-100 in UB buffer (150 mM NaCl, 50 mM Tris, pH 7.6, and 0.01% NaN_3) for 3 min, and washed in UB buffer. Cells were blocked with 10% BSA in UB buffer for E-cadherin talin, paxillin, β-catenin, vinculin, and phospho-Y822 vinculin staining for 30 min at 37°C, incubated with a primary antibody for 45 min at 37°C, washed, and incubated with secondary antibody for 45 min at 37°C. E-cadherin was visualized staining with HECD-1 (EMD Millipore) at a 1:1,000 dilution, followed by Texas red–conjugated goat anti–mouse IgG (H+L) (Jackson ImmunoResearch Laboratories, Inc.) at a 1:500 dilution. Talin (Sigma-Aldrich) was stained for at a 1:300 dilution, followed by Texas red–conjugated goat anti–mouse IgG (H+L) (Jackson ImmunoResearch Laboratories, Inc.) at a 1:500 dilution. Paxillin was visualized using TRITC-conjugated mouse antibody (BD). β-catenin (Sigma-Aldrich) was stained for at 1:1,000 with anti–rabbit Texas red. Vinculin was visualized using a cocktail of hVin-1 (Sigma-Aldrich) and 7F9 (EMD Millipore) at 1:200 and then Texas red–conjugated goat anti–mouse IgG. Phospho-Y822 vinculin (EMD Millipore and then Abcam) was stained for at a 1:50 dilution, followed by Texas red–conjugated anti–rabbit IgG (H+L). Fluorescence images were captured with a confocal microscope (LSM 510; Carl Zeiss). We used a 63×/NA 1.4 oil objective (Carl Zeiss). Images were obtained using LSM Image Browser (Carl Zeiss). Phase images were captured at room temperature with an inverted microscope (Axiovert 200M; Carl Zeiss), equipped with an ORCA-ERA 1394 HD camera (Hamamatsu Photonics). A 10× EC Plan Neofluor objective (NA 0.55; Carl Zeiss) was used for these studies. Images were acquired using Axiovision 4.7 software (Carl Zeiss). For the TEM studies, confluent cells growing on 0.4-µm Transwell filters were fixed in 2.5% glutaraldehyde in 0.1 M cacodylate buffer. After rinses in 0.1 M cacodylate buffer, cells were processed for transmission electron microscopy using routine procedures. Ultrathin sections were cut with an ultramicrotome (EM UC6; Leica) and imaged in a transmission electron microscope (JEM-1230; JEOL USA, Inc.) equipped with a CCD camera (Ultrascan 2k × 2k; Gatan).

Protein purification and in vitro kinase assay

Recombinant GST, GST-vinculin 811–881, and GST-vinculin 811–881 Y822F were purified by affinity chromatography. After elution, proteins were dialyzed against FP buffer (10 mM Tris-HCl, pH 7.6, and 100 mM NaCl). Proteins were concentrated using the Amicon Ultra 30,000 MWCO system (EMD Millipore) and stored at 4°C. 2 µg of purified proteins were incubated in the presence of 20 mM Pipes (pH 7.0), 10 mM $MnCl_2$, 20 µg of aprotinin per ml, and 1 mM ATP for 10 min at 30°C in the presence of purified recombinant Abl kinase (EMD Millipore), with or without 5 µM Gleevec (Alexis). The reaction was stopped by adding an equal volume of 2× sample buffer (10 mM EDTA, 4% SDS, 5.6 mM 2-mercaptoethanol, 20% glycerol, 200 mM Tris-HCl, pH 6.8, and 1% Bromophenol blue). The samples were separated by SDS-PAGE and analyzed by Western blot. The resulting gel was stained to ensure that equal amounts of the purified proteins were present in all samples.

Force microscopy

Three-dimensional force microscopy (3DFM; Fisher et al., 2006) experiments were performed as described previously (Shen et al., 2011) with the following modifications. Tosylactivated magnetic Dynabeads (2.8 µm; Invitrogen) were coated with either fibronectin or Fc-tagged E-cadherin (R&D Systems) according to the manufacturer's protocol. Cells were seeded onto coverslips for 24 h and incubated for 40 min with beads coated with either FcE-cadherin or fibronectin; where indicated, 10 µM Gleevec was added with the beads (Novartis). Upon pulses of force, bead displacements were captured with a high-speed video camera (Jai Pulnix) and tracked using Video Spot Tracker software developed by the Center for Computer Integrated Systems for Microscopy and Manipulation at the University of North Carolina at Chapel Hill (http://cismm.cs.unc.edu). Beads that did not show displacements greater than 10 nm (due to detection resolution of the 3DFM system) were not used for analysis.

Force assays

Cells were grown to 60–70% confluence and incubated with 1.5 mg Dynabeads Protein A (Invitrogen) coated with 10 µg purified Fc–E-cadherin or IgG or 1.5 mg Dynabeads M-280 Tosylactivated (Invitrogen) coated with 10 µg purified fibronectin or poly-l-lysine at for 40 min in the presence or absence of 10 µM Y27632 (Sigma-Aldrich) or 40 uM imatinib (Eton Biosciences) at 37°C. Cells were pervanadate treated and beads were incubated for 5 min with a permanent ceramic magnet that had been calibrated as described previously (Guilluy et al., 2011). In brief, the magnetic beads were placed in a closed well, in fluid of known viscosity, and at a known distance from the face of the permanent magnet. Particle velocities were obtained using Video Spot Tracker and in-house MATLAB programs and applied force was calculated using Stokes' formula. For all experiments, the magnet was placed parallel with and at a distance of 0.6 cm from the cell surface. At this distance the force on a single bead is 10 pN. The cells were transferred to ice and immediately lysed.

Online supplemental material

Fig. S1 shows the specificity of the phospho-Y822 antibody. Fig. S2 shows examination of vinculin phosphorylation in response to cadherin engagement and in response to application of force on E-cadherin. Fig. S3 shows that paxillin recruitment to FAK is unaltered in the Y822F-expressing cell lines. Fig. S4 shows that Y822F does not rescue the epithelial cell–cell junction defects induced by loss of vinculin. Fig. S5 shows that WT and Y822F vinculin co-sediment with actin equally well. Online supplemental material is available at http://www.jcb.org/cgi/content/full/jcb.201309092/DC1.

We thank Lacy Barton, Johanna Uribe, Yuan Pan, and Chaoqun Zheng for the pilot studies they completed that laid the foundation for this work. We also thank Thomas Moninger in the Central Microscopy Facility at the University of Iowa for his assistance with the transmission EM studies.

This work is supported by National Science Foundation grant no. 1120478 (to K.A. DeMali), National Institutes of Health grants 1RO1GM029860 (to K. Burridge) and 5P41EB002025 (to R. Superfine), and American Heart Association Predoctoral Fellowship no. 0910127G (to X. Peng). C. Guilluy is supported by a Marie Curie Outgoing International Fellowship from the European Union Seventh Framework Program (FP7/2007-2013) under grant agreement number 254747.

The authors declare no further competing financial interests.

Author contributions: J.L. Bays, X. Peng, and K.A. DeMali designed and executed experiments, interpreted data and prepared the manuscript. C.E. Tolbert and C. Guilluy executed and interpreted the 3DFM experiments. A.E. Angell and Y. Pan executed experiments. R. Superfine provided access to the equipment necessary to execute the 3DFM experiments. K. Burridge contributed key suggestions and revised the manuscript. All authors provided detailed comments on the manuscript.

Submitted: 18 September 2013
Accepted: 19 March 2014

References

Alenghat, F.J., B. Fabry, K.Y. Tsai, W.H. Goldmann, and D.E. Ingber. 2000. Analysis of cell mechanics in single vinculin-deficient cells using a magnetic tweezer. *Biochem. Biophys. Res. Commun.* 277:93–99. http://dx.doi.org/10.1006/bbrc.2000.3636

Borghi, N., M. Sorokina, O.G. Shcherbakova, W.I. Weis, B.L. Pruitt, W.J. Nelson, and A.R. Dunn. 2012. E-cadherin is under constitutive actomyosin-generated tension that is increased at cell-cell contacts upon externally applied stretch. *Proc. Natl. Acad. Sci. USA*. 109:12568–12573. http://dx.doi.org/10.1073/pnas.1204390109

Bradley, W.D., S.E. Hernández, J. Settleman, and A.J. Koleske. 2006. Integrin signaling through Arg activates p190RhoGAP by promoting its binding to p120RasGAP and recruitment to the membrane. *Mol. Biol. Cell*. 17:4827–4836. http://dx.doi.org/10.1091/mbc.E06-02-0132

Brazzelli, V., V. Grasso, and G. Borroni. 2013. Imatinib, dasatinib and nilotinib: a review of adverse cutaneous reactions with emphasis on our clinical experience. *J. Eur. Acad. Dermatol. Venereol.* 27:1471–1480. http://dx.doi.org/10.1111/jdv.12172

Burton, E.A., R. Plattner, and A.M. Pendergast. 2003. Abl tyrosine kinases are required for infection by Shigella flexneri. *EMBO J.* 22:5471–5479. http://dx.doi.org/10.1093/emboj/cdg512

Calautti, E., S. Cabodi, P.L. Stein, M. Hatzfeld, N. Kedersha, and G. Paolo Dotto. 1998. Tyrosine phosphorylation and src family kinases control keratinocyte cell-cell adhesion. *J. Cell Biol.* 141:1449–1465. http://dx.doi.org/10.1083/jcb.141.6.1449

Chen, C.S., J. Tan, and J. Tien. 2004. Mechanotransduction at cell-matrix and cell-cell contacts. *Annu. Rev. Biomed. Eng.* 6:275–302. http://dx.doi.org/10.1146/annurev.bioeng.6.040803.140040

Chen, Z., E. Lessey, M.E. Berginski, L. Cao, J. Li, X. Trepat, M. Itano, S.M. Gomez, M. Kapustina, C. Huang, et al. 2013. Gleevec, an Abl family inhibitor, produces a profound change in cell shape and migration. *PLoS ONE.* 8:e52233. http://dx.doi.org/10.1371/journal.pone.0052233

Chrzanowska-Wodnicka, M., and K. Burridge. 1996. Rho-stimulated contractility drives the formation of stress fibers and focal adhesions. *J. Cell Biol.* 133:1403–1415. http://dx.doi.org/10.1083/jcb.133.6.1403

DeMali, K.A., C.A. Barlow, and K. Burridge. 2002. Recruitment of the Arp2/3 complex to vinculin: coupling membrane protrusion to matrix adhesion. *J. Cell Biol.* 159:881–891. http://dx.doi.org/10.1083/jcb.200206043

Fisher, J.K., J. Cribb, K.V. Desai, L. Vicci, B. Wilde, K. Keller, R.M. Taylor, J. Haase, K. Bloom, E.T. O'Brien, and R. Superfine. 2006. Thin-foil magnetic force system for high-numerical-aperture microscopy. *Rev. Sci. Instrum.* 77:s8302. http://dx.doi.org/10.1063/1.2166509

Galbraith, C.G., K.M. Yamada, and M.P. Sheetz. 2002. The relationship between force and focal complex development. *J. Cell Biol.* 159:695–705. http://dx.doi.org/10.1083/jcb.200204153

Geiger, B. 1979. A 130K protein from chicken gizzard: its localization at the termini of microfilament bundles in cultured chicken cells. *Cell*. 18:193–205. http://dx.doi.org/10.1016/0092-8674(79)90368-4

Geiger, B., K.T. Tokuyasu, A.H. Dutton, and S.J. Singer. 1980. Vinculin, an intracellular protein localized at specialized sites where microfilament bundles terminate at cell membranes. *Proc. Natl. Acad. Sci. USA*. 77:4127–4131. http://dx.doi.org/10.1073/pnas.77.7.4127

Goldmann, W.H., R. Galneder, M. Ludwig, W. Xu, E.D. Adamson, N. Wang, and R.M. Ezzell. 1998. Differences in elasticity of vinculin-deficient F9 cells measured by magnetometry and atomic force microscopy. *Exp. Cell Res.* 239:235–242. http://dx.doi.org/10.1006/excr.1997.3915

Goldyn, A.M., B.A. Rioja, J.P. Spatz, C. Ballestrem, and R. Kemkemer. 2009. Force-induced cell polarisation is linked to RhoA-driven microtubule-independent focal-adhesion sliding. *J. Cell Sci.* 122:3644–3651. http://dx.doi.org/10.1242/jcs.054866

Grashoff, C., B.D. Hoffman, M.D. Brenner, R. Zhou, M. Parsons, M.T. Yang, M.A. McLean, S.G. Sligar, C.S. Chen, T. Ha, and M.A. Schwartz. 2010. Measuring mechanical tension across vinculin reveals regulation of focal adhesion dynamics. *Nature*. 466:263–266. http://dx.doi.org/10.1038/nature09198

Guilluy, C., V. Swaminathan, R. Garcia-Mata, E.T. O'Brien, R. Superfine, and K. Burridge. 2011. The Rho GEFs LARG and GEF-H1 regulate the mechanical response to force on integrins. *Nat. Cell Biol.* 13:722–727. http://dx.doi.org/10.1038/ncb2254

Hazan, R.B., L. Kang, S. Roe, P.I. Borgen, and D.L. Rimm. 1997. Vinculin is associated with the E-cadherin adhesion complex. *J. Biol. Chem.* 272:32448–32453. http://dx.doi.org/10.1074/jbc.272.51.32448

Huveneers, S., and J. de Rooij. 2013. Mechanosensitive systems at the cadherin-F-actin interface. *J. Cell Sci.* 126:403–413. http://dx.doi.org/10.1242/jcs.109447

Huveneers, S., J. Oldenburg, E. Spanjaard, G. van der Krogt, I. Grigoriev, A. Akhmanova, H. Rehmann, and J. de Rooij. 2012. Vinculin associates with endothelial VE-cadherin junctions to control force-dependent remodeling. *J. Cell Biol.* 196:641–652. http://dx.doi.org/10.1083/jcb.201108120

Irvine, E., and C. Williams. 2013. Treatment-, patient-, and disease-related factors and the emergence of adverse events with tyrosine kinase inhibitors for the treatment of chronic myeloid leukemia. *Pharmacotherapy*. 33:868–881. http://dx.doi.org/10.1002/phar.1266

Kain, K.H., and R.L. Klemke. 2001. Inhibition of cell migration by Abl family tyrosine kinases through uncoupling of Crk-CAS complexes. *J. Biol. Chem.* 276:16185–16192. http://dx.doi.org/10.1074/jbc.M100095200

le Duc, Q., Q. Shi, I. Blonk, A. Sonnenberg, N. Wang, D. Leckband, and J. de Rooij. 2010. Vinculin potentiates E-cadherin mechanosensing and is recruited to actin-anchored sites within adherens junctions in a myosin II-dependent manner. *J. Cell Biol.* 189:1107–1115. http://dx.doi.org/10.1083/jcb.201001149

Lessey, E.C., C. Guilluy, and K. Burridge. 2012. From mechanical force to RhoA activation. *Biochemistry*. 51:7420–7432. http://dx.doi.org/10.1021/bi300758e

Maddugoda, M.P., M.S. Crampton, A.M. Shewan, and A.S. Yap. 2007. Myosin VI and vinculin cooperate during the morphogenesis of cadherin cell cell contacts in mammalian epithelial cells. *J. Cell Biol.* 178:529–540. http://dx.doi.org/10.1083/jcb.200612042

McLachlan, R.W., A. Kraemer, F.M. Helwani, E.M. Kovacs, and A.S. Yap. 2007. E-cadherin adhesion activates c-Src signaling at cell-cell contacts. *Mol. Biol. Cell*. 18:3214–3223. http://dx.doi.org/10.1091/mbc.E06-12-1154

Mierke, C.T., P. Kollmannsberger, D.P. Zitterbart, J. Smith, B. Fabry, and W.H. Goldmann. 2008. Mechano-coupling and regulation of contractility by the vinculin tail domain. *Biophys. J.* 94:661–670. http://dx.doi.org/10.1529/biophysj.107.108472

Niessen, C.M. 2007. Tight junctions/adherens junctions: basic structure and function. *J. Invest. Dermatol.* 127:2525–2532. http://dx.doi.org/10.1038/sj.jid.5700865

Owens, D.W., G.W. McLean, A.W. Wyke, C. Paraskeva, E.K. Parkinson, M.C. Frame, and V.G. Brunton. 2000. The catalytic activity of the Src family kinases is required to disrupt cadherin-dependent cell-cell contacts. *Mol. Biol. Cell*. 11:51–64. http://dx.doi.org/10.1091/mbc.11.1.51

Pasapera, A.M., I.C. Schneider, E. Rericha, D.D. Schlaepfer, and C.M. Waterman. 2010. Myosin II activity regulates vinculin recruitment to focal adhesions through FAK-mediated paxillin phosphorylation. *J. Cell Biol.* 188:877–890. http://dx.doi.org/10.1083/jcb.200906012

Peng, X., L.E. Cuff, C.D. Lawton, and K.A. DeMali. 2010. Vinculin regulates cell-surface E-cadherin expression by binding to beta-catenin. *J. Cell Sci.* 123:567–577. http://dx.doi.org/10.1242/jcs.056432

Place, T.L., J.T. Nauseef, M.K. Peterson, M.D. Henry, J.J. Mezhir, and F.E. Domann. 2013. Prolyl-4-hydroxylase 3 (PHD3) expression is downregulated during epithelial-to-mesenchymal transition. *PLoS One*. 8:e83021. http://dx.doi.org/10.1371/journal.pone.0083021

Plotnikov, S.V., and C.M. Waterman. 2013. Guiding cell migration by tugging. *Curr. Opin. Cell Biol.* 25:619–626. http://dx.doi.org/10.1016/j.ceb.2013.06.003

Riveline, D., E. Zamir, N.Q. Balaban, U.S. Schwarz, T. Ishizaki, S. Narumiya, Z. Kam, B. Geiger, and A.D. Bershadsky. 2001. Focal contacts as mechanosensors: externally applied local mechanical force induces growth of focal contacts by an mDia1-dependent and ROCK-independent mechanism. *J. Cell Biol.* 153:1175–1186. http://dx.doi.org/10.1083/jcb.153.6.1175

Ruoslahti, E., E.G. Hayman, M. Pierschbacher, and E. Engvall. 1982. Fibronectin: purification, immunochemical properties, and biological activities. *Methods Enzymol.* 82:803–831. http://dx.doi.org/10.1016/0076-6879(82)82103-4

Saunders, R.M., M.R. Holt, L. Jennings, D.H. Sutton, I.L. Barsukov, A. Bobkov, R.C. Liddington, E.A. Adamson, G.A. Dunn, and D.R. Critchley. 2006. Role of vinculin in regulating focal adhesion turnover. *Eur. J. Cell Biol.* 85:487–500. http://dx.doi.org/10.1016/j.ejcb.2006.01.014

Sefton, B.M., T. Hunter, E.H. Ball, and S.J. Singer. 1981. Vinculin: a cytoskeletal target of the transforming protein of Rous sarcoma virus. *Cell*. 24:165–174. http://dx.doi.org/10.1016/0092-8674(81)90512-2

Shen, K., C.E. Tolbert, C. Guilluy, V.S. Swaminathan, M.E. Berginski, K. Burridge, R. Superfine, and S.L. Campbell. 2011. The vinculin C-terminal hairpin mediates F-actin bundle formation, focal adhesion, and cell mechanical properties. *J. Biol. Chem.* 286:45103–45115. http://dx.doi.org/10.1074/jbc.M111.244293

Subauste, M.C., O. Pertz, E.D. Adamson, C.E. Turner, S. Junger, and K.M. Hahn. 2004. Vinculin modulation of paxillin-FAK interactions regulates ERK to control survival and motility. *J. Cell Biol.* 165:371–381. http://dx.doi.org/10.1083/jcb.200308011

Sumida, G.M., T.M. Tomita, W. Shih, and S. Yamada. 2011. Myosin II activity dependent and independent vinculin recruitment to the sites of E-cadherin-mediated cell-cell adhesion. *BMC Cell Biol.* 12:48. http://dx.doi.org/10.1186/1471-2121-12-48

Tsai, J., and L. Kam. 2009. Rigidity-dependent cross talk between integrin and cadherin signaling. *Biophys. J.* 96:L39–L41. http://dx.doi.org/10.1016/j.bpj.2009.01.005

Volberg, T., B. Geiger, J. Kartenbeck, and W.W. Franke. 1986. Changes in membrane-microfilament interaction in intercellular adherens junctions upon removal of extracellular Ca^{2+} ions. *J. Cell Biol.* 102:1832–1842. http://dx.doi.org/10.1083/jcb.102.5.1832

Xu, W., H. Baribault, and E.D. Adamson. 1998. Vinculin knockout results in heart and brain defects during embryonic development. *Development*. 125:327–337.

Yonemura, S., Y. Wada, T. Watanabe, A. Nagafuchi, and M. Shibata. 2010. α-Catenin as a tension transducer that induces adherens junction development. *Nat. Cell Biol.* 12:533–542. http://dx.doi.org/10.1038/ncb2055

Zandy, N.L., and A.M. Pendergast. 2008. Abl tyrosine kinases modulate cadherin-dependent adhesion upstream and downstream of Rho family GTPases. *Cell Cycle*. 7:444–448. http://dx.doi.org/10.4161/cc.7.4.5452

Zandy, N.L., M. Playford, and A.M. Pendergast. 2007. Abl tyrosine kinases regulate cell-cell adhesion through Rho GTPases. *Proc. Natl. Acad. Sci. USA*. 104:17686–17691. http://dx.doi.org/10.1073/pnas.0703077104

Zhao, X.H., C. Laschinger, P. Arora, K. Szászi, A. Kapus, and C.A. McCulloch. 2007. Force activates smooth muscle alpha-actin promoter activity through the Rho signaling pathway. *J. Cell Sci.* 120:1801–1809. http://dx.doi.org/10.1242/jcs.001586

Zipfel, P.A., W. Zhang, M. Quiroz, and A.M. Pendergast. 2004. Requirement for Abl kinases in T cell receptor signaling. *Curr. Biol.* 14:1222–1231. http://dx.doi.org/10.1016/j.cub.2004.07.021